α decay of $^{243}Fm_{143}$ and $^{245}Fm_{145}$, and of their daughter nuclei

J. Khuyagbaatar,[1,*] F. P. Heßberger,[1] S. Hofmann,[1] D. Ackermann,[1,2] H. G. Burkhard,[1] S. Heinz,[1] B. Kindler,[1] I. Kojouharov,[1] B. Lommel,[1] R. Mann,[1] J. Maurer,[1] and K. Nishio[3]

[1]*GSI Helmholtzzentrum für Schwerionenforschung, 64291 Darmstadt, Germany*

[2]*GANIL, CEA/DSM-CNRS/IN2P3, Bd Henri Becquerel, BP 55027, F-14076 Caen Cedex 5, France*

[3]*Japan Atomic Energy Agency, Tokai, Ibaraki, 319-1195, Japan*

(Received 26 February 2020; revised 29 July 2020; accepted 22 September 2020; published 12 October 2020)

Nuclear structure of ^{243}Fm, ^{245}Fm, and their daughter nuclei were investigated via detection of their radioactive decays, α, γ, and spontaneous fission. Measured α-decay energies, half-lives, and branching ratios improve the literature data significantly. A signature for detection of the hitherto unknown ^{235}Cm was found in the α-decay chains from ^{243}Fm. Two groups of α events with average energies of 6.69(2) MeV and 7.01(2) MeV and with a half-life of $T_{1/2} = 300^{+250}_{-100}$ s are suggested to originate from ^{235}Cm. Tentative decay schemes for ^{243}Fm, ^{239}Cf, ^{235}Cm, and ^{245}Fm, ^{241}Cf isotopes are suggested based on the present experimental data. Systematical trends of single-particle states in $N = 141$ isotones of $Z = 92$–98 nuclei are discussed.

DOI: 10.1103/PhysRevC.102.044312

I. INTRODUCTION

The properties of microscopic single-particle energy levels determine the interplay between the attractive nuclear and repulsive electric forces. They become most important in the region of heavy and superheavy nuclei, where the stabilizing macroscopic liquid-drop properties vanish [1–7]. Especially large binding energies are expected for spherical nuclei at and near closed shells for either protons and neutrons or both. As a result, these nuclei have relatively long partial spontaneous fission (SF) half-lives due to high fission barriers. Also partial α-decay half-lives are prolonged for nuclei at and below the closed shells.

For many decades, the aim of experimental studies was to confirm the existence of an island of stability predicted to be located at proton number $Z = 114$ and neutron number $N = 184$ [1,3,7–9]. Only in recent years, experimental data confirmed an increase of stability for nuclei with $Z = 114$–118 and neutron numbers approaching the predicted closed shell at $N = 184$ [8]. In addition to the closed shells for protons and neutrons, increased stability was predicted for deformed nuclei with proton and neutron numbers $Z = 100$, $N = 152$ and $Z = 108$, $N = 162$ [3,9,10].

For these proton and neutron numbers large single-particle energy gaps were calculated, which result in increased binding energies due to an increase of the level density below the gap. It was calculated that the width of this energy gap is rather robust and only weakly dependent on the number of the complementary type of nucleons over a relatively wide range. For obtaining the highest stability, not only the quadrupole deformation, which has a value of $\beta_2 \approx 0.25$, but also higher-order degrees of deformation have to be considered. The existence of both regions of increased stability for deformed nuclei is experimentally well established by measurements of partial SF and α-decay half-lives, energies, and spectroscopic data [1,2,5,6,11].

So far not clearly proven is an increased stability predicted for more neutron-deficient deformed nuclei, $\beta_2 \approx 0.22$, located at $Z = 96$–100 and $N = 142$ [9,10]. For these nuclei located at the limit of the presently known isotopes, spectroscopic information is scarce. In particular, systematic trends of binding energies, α-decay energies (E_α) and partial α-decay half-lives (T_α), and spin and parity (I^π) values of ground and excited states are incomplete.

In the present work, we aimed to study the α decay of ^{245}Fm ($N = 145$) and ^{243}Fm ($N = 143$) and their daughter nuclei ^{241}Cf ($N = 143$) and ^{239}Cf ($N = 141$), in order to accumulate information on single-particle neutron states of $N = 141$ and $N = 143$ isotones.

II. EXPERIMENTAL DETAILS

The experimental data were gathered in several shorter irradiations already in 2007 and the data on SF were presented in Ref. [12]. Accordingly, in this work we present the data on the α decay.

The experiment was performed using the velocity filter SHIP at GSI in Darmstadt. The fermium isotopes were produced by the fusion-evaporation reactions ^{40}Ar + ^{206}Pb and ^{40}Ar + ^{208}Pb. The argon beam with a charge state of 9^+ and with an intensity of up to 3 particle μA (1 particle μA = 6.25×10^{12} particles per second) was delivered by the linear accelerator UNILAC. Lead sulfide (PbS) targets with average thicknesses of $\approx$400 μg/cm^2 (for Pb) had been evaporated on carbon backing foils of 40 μg/cm^2 thickness [13]. On the downstream side, the target was covered by a 10 μg/cm^2 carbon layer. The targets were mounted on a wheel, which

*j.khuyagbaatar@gsi.de

rotated synchronously to the beam structure (5 ms long pulses with 50 Hz repetition frequency).

The evaporation residues (ERs) were separated from the primary beam by the velocity filter SHIP [14] and were then implanted into a position sensitive 16-strip Si detector (stop detector) with an active area of 80×35 mm^2 [1]. Before implantation, the ERs passed through two time-of-flight (TOF) detectors [15]. Their signals were also used to distinguish the incoming ERs and radioactive decays of the implanted nuclei.

Six additional silicon detectors of the same size as the stop detector, subdivided into 28 energy-sensitive segments, were mounted in the backward hemisphere for detection of escaped α particles or fission fragments (box detector). These detectors covered an area of 85% of the backward hemisphere. The signals from stop and box detectors were split into two energy ranges; a low-energy 0.2–16.0 MeV and a high-energy branch 4–320 MeV for the stop detector and 2–160 MeV for the box detector. The signals of the low-energy branch were calibrated using α particles of implanted nuclei produced in the nucleon transfer channels of the ^{40}Ar + ^{206,208}Pb reactions. The typical energy resolution of the stop-detector strips was 25 keV (FWHM). For most of the segments of the box detector the energy resolution of α particles reconstructed from the sum of the signals from stop-detector strips and box-detector segments was in the range from 60–120 keV depending on the segment involved. The high-energy branches of the stop and the box detectors were calibrated with standard α and fission sources, ^{239}Pu + ^{241}Am + ^{244}Cm and ^{252}Cf, respectively.

The stop detector had been used in a preceding experiment for transfer-reaction studies that was performed two months earlier. Therefore, α decays originating from the long-lived transfer products were detected during the present experiment as shown in Fig. 1(a). This spectrum was taken two days before the start of the present experiment with the ^{40}Ar + ^{208}Pb reaction. All of the observed α lines were identified as marked in the figure.

A high-purity Ge clover detector consisting of four crystals, each 50 mm in diameter and 70 mm in length, was mounted behind the stop detector. The clover detector was calibrated by using ^{133}Ba and ^{152}Eu sources. The typical energy resolution of each crystal was 1.1 keV (FWHM) at 121 keV. Due to high rates of γ rays during the irradiation, signals from the clover detector were recorded within a 5-μs time interval in coincidence with any event registered in stop and/or box detectors. The time difference between the signals, e.g., between stop and clover detector, was measured with time to amplitude converters (TAC). Detailed descriptions of the experimental setup can be found in Refs. [1,12,16].

Radioactive decays of implanted nuclei were studied in time and spatial correlation analysis between signals from the implantation of ERs, α-like, and fissionlike events [17]. The ER-like events were selected using the coincident TOF signals while α-like and fissionlike events required to be anticoincident to the TOF detectors or occurring during the beam-off periods of 15 ms. Position windows of $\pm$1.2 mm and $\pm$0.5 mm were applied for searching for ER-α and α-α sequences, respectively. In the case of α particles emitted in backward direction, which deposit typically small amount of energies ($<$ 1 MeV) in the stop detector, position windows of $\pm$1.5 mm and $\pm$1.0 mm were used for ER-α and α-α correlations, respectively. Different position windows are used due to the energy-dependent position resolution of the detector. Search times for correlated signals were limited due to an average counting rate of $\approx$0.4 Hz of ER-like background events in the position window of a single strip.

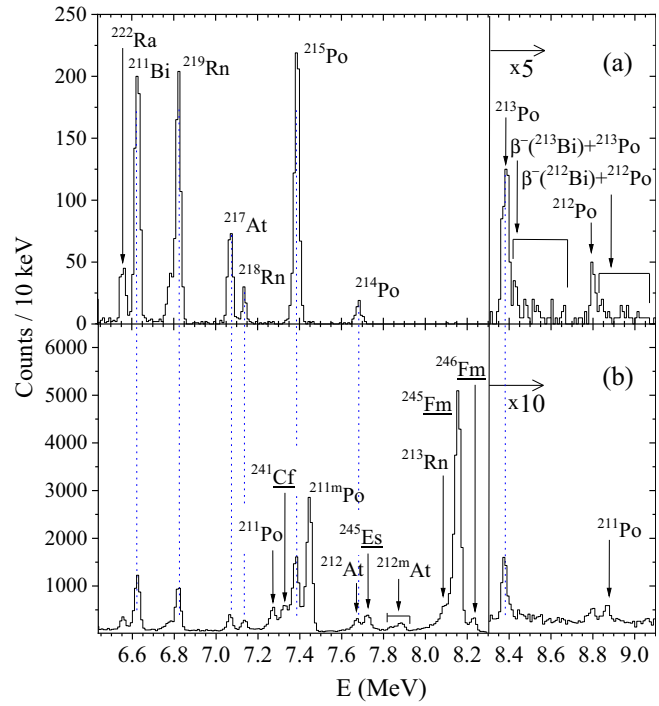

FIG. 1. The stop detector α spectrum from the background measurement taken (a) two days prior to the experiment and (b) from the ^{40}Ar + ^{208}Pb reaction accumulated during the beam-off periods. The identified α lines from background (a), and the ^{40}Ar + ^{208}Pb reaction (b) are indicated. Counts of the events with energies above 8.3 MeV were multiplied by a factors of five and ten in (a) and (b), respectively. Vertical dotted lines mark the energies of the background α lines. See text for details.

III. EXPERIMENTAL RESULTS AND DISCUSSION

A. Decay of ^{245}Fm and its daughter nuclei

The isotope ^{245}Fm was produced in the 3n evaporation channel of the fusion reaction ^{40}Ar + ^{208}Pb at a beam energy of $E_{\rm lab} = 192$ MeV determined at half of the target thickness. This energy corresponds to an excitation energy of 32 MeV of the compound nucleus ^{248}Fm. The α spectrum measured during the beam-off periods is shown in Fig. 1(b). α lines originating from the reaction ^{40}Ar + ^{208}Pb are marked by their corresponding isotope. In the case of lines originating from fusion evaporation, the isotope is underlined. In all other cases the α lines were assigned to transfer reactions.

Identification of α decays from ^{245}Fm and its daughters by correlation analysis (ER-α and/or α-α) was not possible due to a high contribution from background events having similar properties as the ^{245}Fm ER's. The measured rate of

0.4 Hz of these events within the used position window was 70 times larger than the rate of ^{245}Fm ER's. For this reason, a sufficiently long correlation time could not be applied, which should exceed at least three times the half-life of 4.2(13) s of ^{245}Fm [18]. Therefore, α decays of the fusion-evaporation products were identified by their well-known decay properties [19–22]. The most intense α peak at an energy of 8.155(7) MeV corresponds to the decay of ^{245}Fm. A cross-section value of 32(3) nb was deduced from the number of detected α events. The decay of ^{241}Cf, which was produced after the α decay of ^{245}Fm is visible at an energy of 7.328(15) MeV. No other α transitions and/or fission events were attributed to ^{241}Cf and ^{245}Fm. α-decay branches of 0.15(1) and ≈1, respectively, were obtained. The new value for ^{241}Cf significantly improves the literature data of ≈0.25 [23,24].

The α line at the energy of 7.73 MeV was assigned to ^{245}Es. This isotope could be produced in the p2n channel of the fusion-evaporation reaction and/or in the electron-capture (EC) decay of ^{245}Fm. A cross-section value of ≈2 nb was deduced from the intensity of the 7.73-MeV line. According to HIVAP calculations [25], the cross section of the p2n channel was expected to be ≈1 nb, which is similar to the experimental value. Thus, the reasonable origin of the ^{245}Es decay is direct production in the p2n fusion-evaporation channel of the $^{40}Ar + ^{208}Pb$ reaction. However, we do not exclude a contribution of a possible EC decay of ^{245}Fm. Based on the number of observed ^{245}Es decays an upper limit of 0.07 was deduced for the EC decay of ^{245}Fm. For the SF branching of ^{245}Fm an upper limit of 0.003 was deduced based on the numbers of observed fission and α events.

α decay of ^{237}Cm, which has an energy of 6.66 MeV and an upper limit of the α-decay branching ratio of 0.01 [26], was impossible to disentangle in the α spectrum. Moreover, it was also not possible to identify the α decay of ^{237}Cm in a triple α correlation sequence due to its long half-life.

Electromagnetic transitions originating from excited and/or isomeric states in the nuclei of interest were searched for by coincident (within ≈5 μs) γ signals in all ER-like and α-like events. Only α-like events were accompanied by such γ rays, which form several peaks clearly distinct from background. An energy spectrum of these γ rays is shown in Fig. 2 together with a two-dimensional spectrum of coincident γ and α events. Three well-pronounced peaks or clusters of the data in the two-dimensional spectrum are visible at γ energies of 50(1), 63(1), 440(1) keV.

We assign the 63-keV γ rays, which are promptly coincident to α particles at ≈7.83 MeV and ≈7.61 MeV to the decay of the first excited level in ^{208}Bi. This 63-keV level is populated in the α decay of the isomeric state ($T_{1/2}$ = 0.12 s, $I^\pi = 9^-$, E_α = 7.837(6) MeV, b_α = 0.66) and of the ground state ($T_{1/2}$ = 0.31 s, $I^\pi = 1^-$, E_α = 7.616(6) MeV, b_α = 0.16) of ^{212}At [23,24].

The 440-keV γ rays were measured within the coincidence window of 5 μs prior to α particles with an energy of ≈8.39 MeV. These γ-α delayed coincidences are assigned to the β^- decay of ^{213}Bi ($T_{1/2}$ = 46 min), which populates a 440-keV level in ^{213}Po with an intensity of 0.31. After γ decay of this level the ^{213}Po ground-state decays by emission of α particles with $T_{1/2}$ = 4.2 μs [23,24].

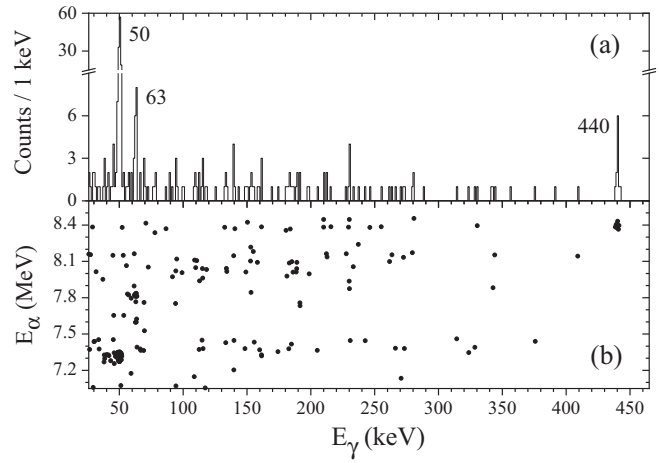

FIG. 2. (a) γ spectrum in coincidence with beam-off α events with stop-detector energies of 7.2–8.5 MeV. (b) Two-dimensional energy spectrum of α particles and coincident γ rays. Energies (in keV) of identified γ lines being in coincidence with α decays are marked. See text for details.

γ rays with an energy of 50(1) keV, which were detected in prompt coincidence to the α decay of ^{241}Cf ($T_{1/2}$ = 227 s, E_α = 7.342(5) MeV, $b_\alpha \approx 0.25$, [23,24]) were not reported previously. Their origin is assigned to the deexcitation of an excited state in ^{237}Cm. A total conversion coefficient of $\alpha_{tot} = 0.21(7)$ was deduced for the 50-keV electromagnetic transition. It was obtained as ratio of the number of measured 50-keV γ rays being in coincidence with 7.328-MeV α particles to the total number of measured 7.328-MeV α particles. The ratio was divided by the efficiency for detection of 50-keV γ rays, which was derived from α-γ coincidences of known transitions of ^{211}Po and ^{212m}At nuclei as described in Ref. [16].

B. Suggested decay schemes for ^{245}Fm, ^{241}Cf, and ^{237}Cm

Decay schemes of ^{245}Fm, ^{241}Cf, and ^{237}Cm are shown on the right side of Fig. 3. The present and literature data [18,23,24,27] were used for the construction of these decay schemes.

α decay of ^{245}Fm with an energy of 8.155(7) MeV is assigned to the favored transition between the single-particle neutron states in mother and daughter nucleus. This assignment is based on a deduced hindrance factor (HF) of 1 for this α transition. The hindrance factor was calculated as a ratio between the measured half-life and that of a semiempirical one estimated from Refs. [28,29] with the present experimental Q_α value.

From the systematics of the known lighter $N = 145$ and 143 isotones, such a favored transition occurs between $1/2^+[631]$ states as the ground-state configuration for the nucleus with $N = 145$ and an excited state for its daughter with $N = 143$. Thus, the above α transition is assigned to the ground-state decay of ^{245}Fm, which populates an excited state with the same $1/2^+[631]$ configuration in ^{241}Cf. To the ground state of ^{241}Cf a $7/2^-[743]$ configuration was attributed based on the systematics of lighter $N = 143$ isotones. Com-

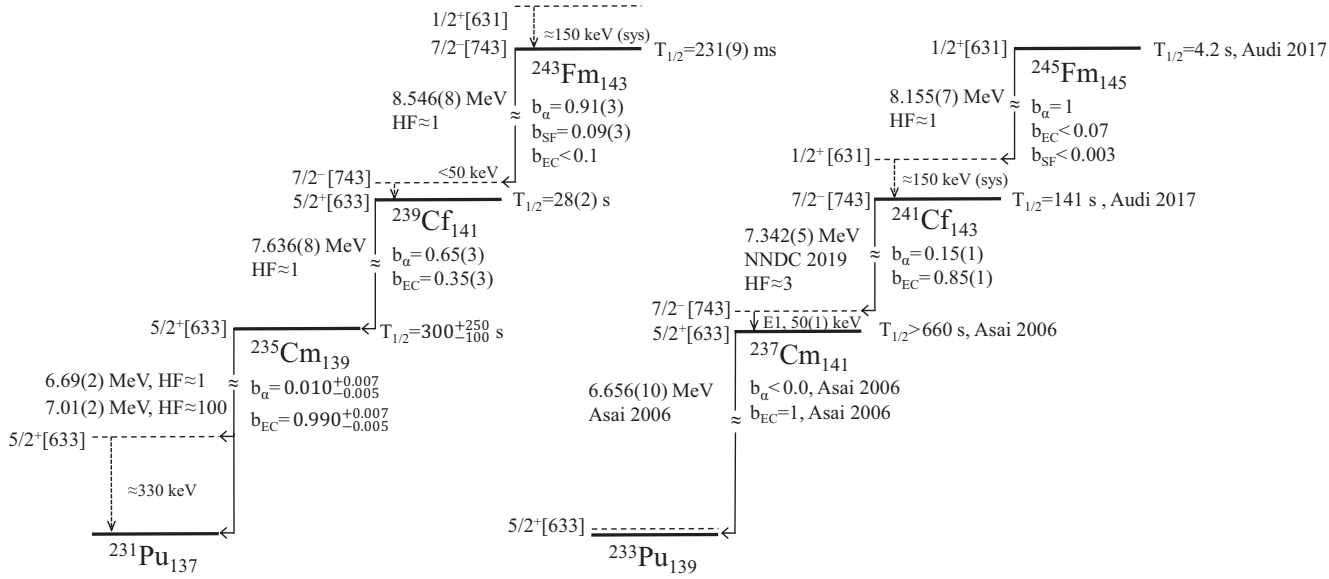

FIG. 3. Suggested decay schemes for isotopes stemming from α decays of ^{243}Fm and ^{245}Fm. The major part of the experimental data (α-decay energies, hindrance factors, branching ratios, and half-lives) is from the present work while literature values are from NNDC 2019 [23], Asai 2006 [26], and Audi 2017 [18]. Dashed lines mark levels assigned tentatively. See text for details.

paring the evaluated ground-state to ground-state α-decay Q value of 8.44(10) MeV for ^{245}Fm [27] and the one of 8.29 MeV deduced from the measured α energy, an excitation energy of ≈150 keV is expected for the $1/2^+[631]$ state in ^{241}Cf. Decay into the $7/2^-[743]$ ground state would occur by a highly L converted $E3$ transition for which a half-life of 0.2 ms is expected according to Weisskopf estimate [24] as known for the cases of the lighter $N = 143$ isotones [23]. In the present experiment, neither α decay nor γ emission of such a long-lived isomeric state could be observed.

With the spin and parity assignments given in Fig. 3, the ground-to-ground state α transition from ^{245}Fm to ^{241}Cf occurs with a change of the angular momentum of $\Delta l = 3$. For such a transition and an α energy of ≈8.3 MeV, we determined a partial α half-life of 3.8 s according to the WKB theory. For details of the used WKB calculation, see Ref. [30]. A similar calculation for the ground-to-excited state decay results in a partial α half-life of 4.6 s for a $\Delta l = 0$ transition and an α energy of 8.155 MeV. Under these conditions we would expect similar intensities of the two transitions. However, we did not observe a clear indication for a ground-to-ground state α decay with an energy of ≈8.3 MeV. From the number of α events within the energy range of 8.25–8.35 MeV an upper limit of 0.02 for the branching ratio of the α decay of the ^{245}Fm ground state to the ground state of ^{241}Cf was deduced. This value results in a lower limit of the partial α half-life of 210 s, which in turn leads to a hindrance factor by nuclear structure of HF > 55 for this transition. The good agreement between measured and calculated half-lives for the transition from the ground to the excited state, on the other hand, results in a hindrance factor of ≈1.

For the α decay of ^{241}Cf, a hindrance factor of HF ≈3 was deduced from the present data. Similar favored α transitions with HF ≈3 are known in the lighter $N = 143$ isotones where they proceed between the $7/2^-[743]$ states. Thus, we suggest that the 7.328-MeV α transition populates an excited state with the $7/2^-[743]$ configuration in the daughter nucleus ^{237}Cm, which predominantly deexcites via emission of a 50-keV γ ray. In Fig. 3, the more precisely measured value of 7.342(5) MeV [23] is given instead of the present result of 7.328(15) MeV.

The experimentally deduced total conversion coefficient is 0.21(7). According to the Weisskopf estimation [24], a 50-keV γ transition decaying within 1 μs can have a multipolarity of either $E1$, $E2$, or $M1$ [24]. Expected conversion coefficients are 0.9, 504, and 52, respectively [31]. Only a multipolarity of $E1$ is in agreement with the experimental value. Therefore, this 50-keV γ is interpreted as an $E1$ transition between the excited $7/2^-[743]$ state and the $5/2^+$ ground state in ^{237}Cm. From these findings, one can deduce a Q_α value of 7.50(2) MeV. This value is in agreement with an evaluated ground-state to ground-state Q_α value of 7.66(15) MeV [27], thus supporting the suggested decay scheme shown in Fig. 3. Based on the systematics of ground-state properties in the lighter $N = 141$ isotones ^{231}Th, ^{233}U, and ^{235}Pu, a $5/2^+[633]$ configuration was attributed to the ground state of ^{237}Cm [26]. The ground-state decay properties of ^{245}Fm and ^{241}Cf are summarized in Table I.

C. Decay of ^{243}Fm and its daughter nuclei

The isotope ^{243}Fm was produced in the ^{40}Ar + ^{206}Pb reaction at beam energies in the range of $E_{\rm lab} = (185–204)$ MeV [12]. The α spectrum measured during the beam-off periods is shown in Fig. 4. Several new peaks compared to the background spectrum shown in Fig. 1(a) were observed. Some of them are due to transfer reactions similar as in the case of the ^{40}Ar + ^{208}Pb reaction [cf. Figs. 1(b) and 4(a)]. Two α lines at energies of 8.546(8) MeV and 7.636(8) MeV corresponding to ^{243}Fm and ^{239}Cf, respectively, are associated

TABLE I. Summary of the present experimental data on α decays and half-lives of the nuclei investigated in this work. The literature half-life values from Refs. [18,23] are also given.

	E_α	$T_{1/2}$		b_α
Isotope	(MeV)	this work	lit.	this work
^{245}Fm	8.155(7)	–	4.2(13) s	1
^{243}Fm	8.546(8)	231(9) ms	–	0.91(3)
^{241}Cf	7.342(5) [23]	–	141(11) s	0.15(1)
^{239}Cf	7.636(8)	28(2) s	39^{+37}_{-12} s	0.65(3)
^{235}Cm	6.69(2)	300^{+250}_{-100} s	–	$0.010^{+0.007}_{-0.005}$
	7.01(2)		–	

with a fusion-evaporation reaction. α-, fission-, and EC-decay branches of 0.91(3), 0.09(3), and <0.1, respectively, of ^{243}Fm were already reported in Ref. [12]. Also reported in Ref. [12] was the lifetime of 333(13) ms [$T_{1/2}$ = 231(9) ms], which was deduced from the time distribution of the $\alpha(^{243}Fm)$ events correlated with their ERs shown in Fig. 5(a). Due to this short half-life, the correlation analysis could be prolonged

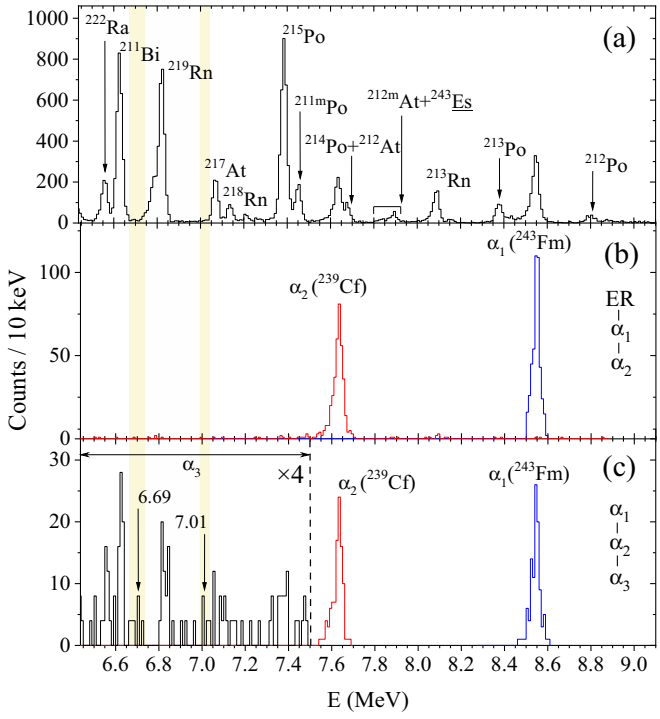

FIG. 4. (a) The α spectrum measured in the stop detector during the beam-off periods from the $^{40}Ar + ^{206}Pb$ reaction. (b) Stop and stop + box detector energies of α_1 and α_2 from the ER–$\alpha_1(^{243}Fm)$–α_2 (6.4–9.0 MeV) correlation. (c) Stop and stop + box detector energies of α_1, α_2, and α_3 from the $\alpha_1(^{243}Fm)$–$\alpha_2(^{239}Cf)$–α_3(6.4–7.5 MeV) correlation. Counts in the energy range of α_3 were multiplied by a factor of four. Shaded rectangles mark the regions where the energies of the α_3 events do not overlap with energies of the background α peaks. α lines originating from transfer reactions are marked by the corresponding isotope in (a). α lines of the fusion-evaporation product ^{243}Fm, its α-decay daughter ^{239}Cf, and its granddaughter ^{235}Cm are marked by the isotope or α energy, respectively, in (b) and (c). For details see text.

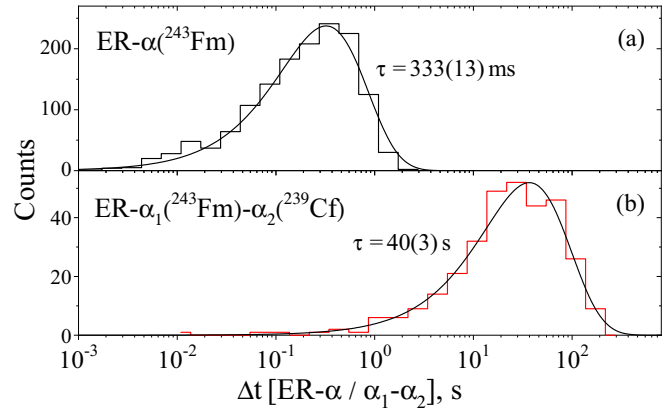

FIG. 5. (a) The time distribution of the α events from the ER–α (^{243}Fm) sequence taken from Ref. [12]. (b) The time distribution α_1–α_2 from the ER–α_1 (^{243}Fm)–α_2 sequence measured here (signals from stop detector and sum of signals from stop and box detectors were considered) is attributed to the decay of ^{239}Cf. Solid lines correspond to the fit of the experimental data with lifetimes of τ = 333(13) s and τ = 40(3) s, respectively, according to Ref. [33].

in order to search for additional α events. Here we present the data on the decays of the daughter isotope ^{239}Cf and the granddaughter ^{235}Cm.

A correlation analysis searching for an ER–$\alpha_1(^{243}Fm)$–α_2 (6.4–9.0 MeV) sequence was performed to identify the α decay of ^{239}Cf [22]. The search time for the α_2 member was set to 200 s and only beam-off events were requested. The energy spectra of the α_1 and α_2 members found from the triple correlation are shown in Fig. 4(b). Only one group of α particles with an energy of 7.636(8) MeV was found to follow the decay of ^{243}Fm. It was assigned to the decay of ^{239}Cf.

The time distribution of the α_2 events at 7.636(8) MeV is shown in Fig. 5(b). The figure shows a representation of an exponential decay curve using logarithmically increasing time bins. To our knowledge this representation was first published in Ref. [32]. For the calculation of the error bars in the case of poor statistics and the determination of true and accidental correlation chains we used the methods worked out in Ref. [33]. From a fit of the time distribution, a lifetime of τ = 40(3) s that corresponds to $T_{1/2}$ = 28(2) s was deduced, which significantly improves the literature value of $T_{1/2} = 39^{+37}_{-12}$ s [22,23]. An α-decay branching of 0.65(3) was determined based on the measured numbers of α decays of ^{243}Fm and ^{239}Cf [cf. Fig. 4(a)]. No γ line was found, which could be attributed to ^{243}Fm and/or ^{239}Cf. In addition, we searched for a third α-decay member (^{235}Cm) in the α-decay chains originating from ^{243}Fm by performing the correlation analysis of $\alpha_1(^{243}Fm)$–$\alpha_2(^{239}Cf)$–α_3 (6.4–7.5 MeV).

We note that our first attempt to identify the decay of ^{235}Cm was carried out already in 2006 [35]. In that work, we used the $^{30}Si + ^{208}Pb$ reaction in which ^{235}Cm was directly produced in a 3n-evaporation channel. We have observed four and two α-decay chains, which had energies of 6.67(2) MeV and 6.98(2) MeV for the first α decays, respectively. The second, third, and fourth α decays had similar properties as the decays of ^{231}Pu, ^{227}U, and ^{223}Th, respectively, as expected for a decay of the parent ^{235}Cm. However, we could not measure the

correlation times for the first events because of the high random probabilities of the ER-like signals. Thus, for confirmation of these results we needed an additional experiment where the half-life of ^{235}Cm could be measured, which was not possible in Ref. [35].

Taking into account a predicted half-life of 300 s for ^{235}Cm [18], a search time of up to 2000 s was chosen for the α_3 member. Energy spectra of the α-decay chain members found in the correlation analysis are shown in Fig. 4(c).

The α_3 events with a broad energy distribution below 7.5 MeV may belong to randomly correlated events and genuine α decays of ^{235}Cm. One can see that the energies of most of the α_3 events coincide with the intense background α lines. Thus, these are attributed to random correlations.

In addition, some α_3 events with average energies of 6.69(2) MeV (five) and 7.01(2) MeV (two) in the stop detector, which are out of the energy range of background α lines are observed. These energies are the same as those we saw in the previous experiment as mentioned above. Thus, presently observed events may belong to the decay of ^{235}Cm.

In order to confirm this assumption, we searched for true and randomly correlated α_3 events at these energies. A triple correlation analysis was performed to search for α_3 events with energies in the ranges of 6.66–6.71 MeV and 6.97–7.02 MeV. The correlation time was prolonged to 10^4 s. The results are shown in Figs. 6(a) and 6(b). Additional two and four α_3 events within the energy ranges of 6.66–6.71 MeV and 6.97–7.02 MeV, respectively, were found with correlation times between 2000 s and 10^4 s.

To examine a random origin of these events a triple correlation was performed for α_3 events with energies in the range of 6.60–6.65 MeV (^{211}Bi), which should occur randomly. The result is shown in Fig. 6(c). An increasing trend of the observed number of events as a function of the correlation time up to 10000 s is observed. This time distribution can be described by an exponential curve with an average correlation time of $\tau_R = 14500$ s. This value was extracted from the events observed in the time windows of 1–2000 s and 2000–10^4 s. The expected number of events within a chosen time window was calculated by considering that the extracted curve with $\tau_R = 14500$ s describes a density distribution of random events according to Refs. [33,34].

For the total number of random events we calculated a value of $N_{\mathrm{R,tot}} = 110$, which results in $N_{\mathrm{R,cal}} = 14$ and 41 random events in the time intervals 1–2000 s and 2000–10^4 s, respectively. These numbers are in agreement with the observed 14 and 43 random events. Assuming that this random time distribution of high counting rate events is valid also for low counting rate events, we calculated the expected total numbers of random events for α_3 (6.66–6.71 MeV) and α_3 (6.97–7.02 MeV) using as basis the observed two and four events, respectively, in the time range from 2000–10^4 s. Expected time distributions of random correlations for α_3 (6.66–6.71 MeV) and α_3 (6.97–7.02 MeV) are shown by the dashed curves in Figs. 6(a) and 6(b), respectively. We expect a total of 6 and 11 random events, respectively. With these numbers, we expect to observe about one randomly correlated event with a correlation time shorter than 2000 s for α_3 (6.66–6.71 MeV). We observed a considerably larger number of

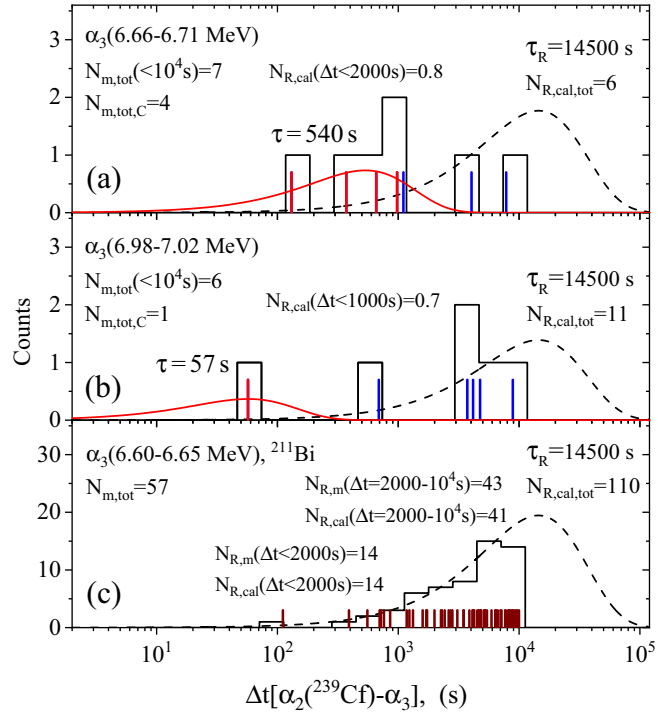

FIG. 6. Time distributions α_2–α_3 from the α_1(^{243}Fm)–α_2(^{239}Cf)–α_3 sequence with energies of 6.69(2) MeV and 7.01(2) MeV are plotted in (a) and (b), respectively. The time distribution of randomly occurring α_3 events from the background α decay of ^{211}Bi is plotted in (c). Only α's measured in the stop detector were considered and the correlation search time was limited to $\Delta t = 10^4$ s. Vertical lines mark the measured individual time Δt between α_2–α_3. Total numbers, $N_{\mathrm{m,tot}}$, of observed events with $\Delta t < 10^4$ s are given. The solid curve in (a) was fitted [33] to the measured four events, which are assigned to a nonrandom correlation ($N_{\mathrm{m,tot,C}}$). The curve with $\tau = 57$ s represents the decay curve based on one correlated event in (b). Dashed curves show the time distribution of the random events with an average correlation time of 14500 s. Calculated values for total numbers of random events, $N_{\mathrm{R,cal,tot}}$, and numbers of events, $N_{\mathrm{R,cal}}$, within various ranges of Δt are given. Measured numbers of random events, $N_{\mathrm{R,m}}$, are also given. See text for the analysis of the data.

five events. Thus, the majority of these events can be considered as nonrandom correlations of the α_1(^{243}Fm)–α_2(^{239}Cf) sequence. We attribute the four events with shorter correlation times to true correlations. The time distribution of these events result in a lifetime of $\tau = 540$ s ($T_{1/2} = 370$ s).

The two correlated events α_3 (6.97–7.02 MeV) were measured at correlation times of 57 and 690 s. For the number of random events having time intervals smaller than 1000 s we calculated a value of 0.7. We attribute the one event observed with the shorter correlation time ($\tau = 57$ s) to be nonrandomly correlated to the α_1(^{243}Fm)–α_2(^{239}Cf) sequence.

Finally, from the total of five α_3 events we determined a half-life of $T_{1/2} = 300^{+250}_{-100}$ s. However, it is necessary to mention that at such a long correlation time and at the present background conditions the correlation analysis could be contaminated by random events. The energies and relative intensities are similar as reported in Ref. [35], which supports

the previous tentative assignment of the two lines to ^{235}Cm. Additional support comes from the predicted α decay Q value of ^{235}Cm of 7.3(2) MeV [27], which is in agreement with the present result within uncertainty. From the intensities of the ^{239}Cf and ^{235}Cm α decays we determined an α-decay branching ratio of $0.010^{+0.007}_{-0.005}$ for ^{235}Cm.

D. Suggested decay schemes for ^{243}Fm, ^{239}Cf, and ^{235}Cm

Tentative decay schemes for ^{243}Fm, ^{239}Cf, and ^{235}Cm are shown on the left in Fig. 3. We did not observe any γ rays associated with the implantation of ^{243}Fm. However, this does not exclude the existence of a $1/2^+[631]$ isomeric state in ^{243}Fm similar to known cases of the lighter $N = 143$ isotones [23] and expected in ^{241}Cf.

A hindrance factor of 1 was calculated for the α decay of ^{243}Fm, which can be attributed to a transition between $7/2^-[743]$ states in ^{243}Fm and ^{239}Cf. For this transition no prompt γ rays were found. This indicates either a change in the ordering of the $7/2^-[743]$ and $5/2^+[633]$ levels or that they are very close in energy (with respect to the lighter $N = 141$ isotone ^{237}Cm). In the suggested decay scheme, a scenario is given, where the ground state of ^{239}Cf has a $5/2^+[633]$ configuration. Consequently, it is suggested that this state decays by emission of α particles with an energy of 7.636(8) MeV, which populates the ground state of ^{235}Cm having the same $5/2^+[633]$ configuration. The latter inference is based on the deduced hindrance factor of 1 and the evaluated Q_α value of 7.81(6) MeV for a ground-to-ground state α transition [27].

Hindrance factors of $\approx$1 and $\approx$100 were deduced for the 6.69(2) MeV and 7.01(2) MeV transitions, respectively. However, we note that uncertainties of these values are large. An estimation based on the numbers of four and one events give $1.0^{+0.8}_{-0.5}$ and 100^{+230}_{-83}, which, nevertheless, indicates that the origin of these two transitions is different. A suggested tentative decay scheme for ^{235}Cm is shown in Fig. 3. The ground-state decay properties of ^{243}Fm, ^{239}Cf, and ^{235}Cm are summarized in Table I.

E. Single-particle neutron levels in $N = 141$ isotones

A single-particle neutron level at $N = 141$ is the most relevant orbital that is filled once the nucleus has 142 neutrons. In Fig. 7, the systematics of the single-particle configurations of the ground and excited states are shown for $N = 141$ isotones. In the present work, we observed an $E1$ transition in ^{237}Cm, which is suggested to originate from deexcitation of the $7/2^-[743]$ state that is populated in the α decay of the mother nucleus ^{241}Cf ($N = 143$). Such favored α transitions are known to occur in lighter $N = 143$ isotones, where the excited $7/2^-[743]$ state in daughter $N = 141$ isotones deexcites via either fast $M1$ or $E1$ transitions as shown in Fig. 7.

Ground states of ^{231}Th, ^{233}U, and ^{235}Pu isotopes are known to have a $5/2^+[633]$ configuration. Based on these facts and taking into account the present results, the same configuration is attributed to ground states of ^{237}Cm, ^{239}Cf, and ^{241}Fm. The lowest-lying single-particle neutron state in ^{231}Th and ^{233}U isotopes appears at excitation energies of 0.18 MeV and 0.28 MeV, respectively. The single-particle levels, next higher

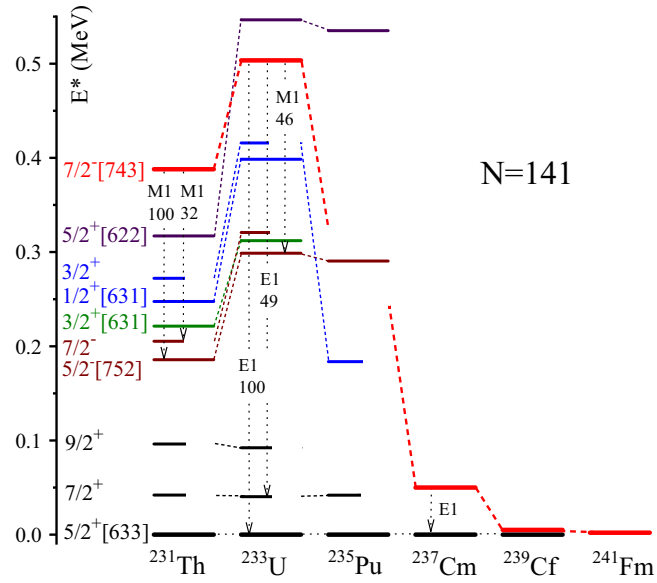

FIG. 7. Low-lying single-particle neutron levels of $N = 141$ isotones known from experiment [23,24] and deduced from systematics [12,18]. Multipolarity and relative intensity of the most intense γ transitions from the deexcitation of the $7/2^-[743]$ states, which are populated in favored α transitions from $N = 143$ nuclei are also given. Short horizontal lines indicate the rotational band members of a certain configuration. Data from ^{237}Cm and ^{239}Cf were obtained in this work. For details see text.

in energy, appear with lower spacing in excitation energy, hence at a higher level density. Furthermore, excitation energies of all single-particle neutron states show an increase from ^{231}Th to ^{233}U. Continuation of such increasing trend of excitation energies as a function of the proton number would indicate the presence of an energy gap at $N = 142$. However, suggested single-neutron configurations of the low-lying excited states in ^{235}Pu show that such an increase does not occur for the $5/2^-[752]$ and $5/2^+[622]$ levels. Their energies are slightly decreased. More interestingly, the tentatively assigned $3/2^+$ state, which is the member of a band with $1/2^+[631]$ configuration shows significant decrease in the energy. Presently suggested configurations for the single-neutron $7/2^-[743]$ level in ^{237}Cm and ^{239}Cf show a steep decrease in the energy compared to lighter ^{233}U. However, one can suggest that in ^{235}Pu the $7/2^-[743]$ level could already be lowered by an energy similar to the case of the $3/2^+$ state. We note that a sudden decrease in excitation energies of both $1/2^+[631]$ and $7/2^-[743]$ states in ^{235}Pu and ^{237}Cm, respectively, could be initiated by a strong change in the nucleus's deformation. This phenomenon could have an interesting, but not well understood, reason [5]. The other $5/2^-[752]$ and $5/2^+[622]$ levels in ^{235}Pu are seemingly not much affected by a variation of such a deformation.

IV. SUMMARY AND CONCLUSION

The radioactive decays of neutron-deficient isotopes stemming from α decays of ^{243}Fm and ^{245}Fm were studied. The present experimental data significantly improve the literature values. Two groups of α decays with average energies of

6.69(2) MeV and 7.01(2) MeV, and with a half-life of $T_{1/2} = 300^{+250}_{-100}$ s are suggested to originate from the decay of hitherto unknown ^{235}Cm. Based on the new and improved experimental data, decay schemes for ^{243}Fm, ^{239}Cf, ^{235}Cm, and ^{245}Fm, ^{241}Cf are established. Systematic trends of low-lying neutron single-particle states in $N = 141$ isotones are discussed.

ACKNOWLEDGMENTS

We thank the UNILAC staff and the ion-source crew for delivering high-intensity and stable beams. We are grateful to J. Steiner, A. Hübner, and to the late W. Hartmann for production of the large area targets and preparation of the target wheels.

[1] S. Hofmann and G. Münzenberg, Rev. Mod. Phys. **72**, 733 (2000).
[2] M. Leino and F. P. Heß berger, Ann. Rev. Nucl. Part. Sci. **54**, 175 (2004).
[3] A. Sobiczewski and K. Pomorski, Prog. Part. Nucl. Phys. **58**, 292 (2007).
[4] O. Sorlin and M.-G. Porquet, Prog. Part. Nucl. Phys. **61**, 602 (2008).
[5] M. Asai, F. P. Heß berger, and A. Lopez-Martens, Nucl. Phys. A **944**, 308 (2015).
[6] D. Ackermann and Ch. Theisen, Phys. Scr. **92**, 083002 (2017).
[7] Yu. Ts. Oganessian, A. Sobiczewski, and G. M. Ter-Akopian, Phys. Scr. **92**, 023003 (2017).
[8] Yu. Ts. Oganessian and V. K. Utyonkov, Nucl. Phys. A **944**, 62 (2015).
[9] P. Möller *et al.*, At. Data Nucl. Data Tables **66**, 131 (1997).
[10] R. R. Chasman, I. Ahmad, A. M. Friedman, and J. R. Erskine, Rev. Mod. Phys. **49**, 833 (1977).
[11] J. Khuyagbaatar *et al.*, Phys. Rev. Lett. **112**, 172501 (2014).
[12] J. Khuyagbaatar *et al.*, Eur. Phys. J. A **37**, 177 (2008).
[13] B. Lommel *et al.*, Nucl. Instrum. Meth. A **480**, 16 (2002).
[14] G. Münzenberg *et al.*, Nucl. Instrum. Meth. **161**, 65 (1979).
[15] S. Saro *et al.*, Nucl. Instrum. Meth. A **381**, 520 (1996).
[16] F. P. Heßberger *et al.*, Eur. Phys. J. A **43**, 55 (2010).
[17] S. Hofmann *et al.*, Nucl. Instrum. Meth. A **223**, 312 (1984).
[18] G. Audi *et al.*, Chin. Phys. C **41**, 030001 (2017).
[19] M. Nurmia *et al.*, Phys. Lett. B **26**, 78 (1967).
[20] Yu. Ts. Oganessian *et al.*, Nucl. Phys. A **239**, 353 (1975).
[21] H. W. Gäggeler *et al.*, Z. Phys. A **289**, 415 (1979).
[22] G. Münzenberg *et al.*, Z. Phys. A **302**, 7 (1981).
[23] http://www.nndc.bnl.gov/ensdf/.
[24] *Table of Isotopes*, edited by R. B. Firestone, 8th ed. (Wiley, New York, 1996).
[25] W. Reisdorf, Z. Phys. A **300**, 227 (1981).
[26] M. Asai *et al.*, Phys. Rev. C **73**, 067301 (2006).
[27] M. Wang *et al.*, Chin. Phys. C **41**, 030003 (2017).
[28] D. N. Poenaru, M. Ivaşcu, and D. Mazilu, J. Phys. Lett. **41**, 589 (1980).
[29] E. Rurarz, Acta Phys. Pol. B **14**, 917 (1983).
[30] S. Hofmann *et al.*, Eur. Phys. J. A **48**, 62 (2012).
[31] T. Kibedi *et al.*, Nucl. Instrum. Meth. A **589**, 202 (2008).
[32] H. Bartsch *et al.*, Nucl. Instrum. Meth. **121**, 185 (1974).
[33] K.-H. Schmidt *et al.*, Z. Phys. A **316**, 19 (1984).
[34] K.-H. Schmidt, Eur. Phys. J. A **8**, 141 (2000).
[35] J. Khuygbaatar *et al.*, GSI Report **2007-1**, 138 (2007).